J. Chem. Sci. Vol. 129, No. 10, October 2017, pp. 1559–1569.
DOI 10.1007/s12039-017-1363-6

REGULAR ARTICLE

A new Co(III) complex of Schiff base derivative for electrochemical recognition of nitrite anion

HAKAN YILMAZ[a,*], ABDULKADIR KOCAK[b], MAOWULIDAN DILIMULATI[a], YUNUS ZORLU[b] and MUBERRA ANDAC[a,*]

[a]Department of Chemistry, Ondokuz Mayis University, 55139 Samsun, Turkey
[b]Department of Chemistry, Gebze Technical University, 41400 Kocaeli, Turkey
E-mail: hakan.yilmaz@omu.edu.tr; mandac@omu.edu.tr

MS received 13 May 2017; revised 7 August 2017; accepted 9 August 2017; published online 19 September 2017

Abstract. The synthesis and characterization of a new Co(III) complex of a salphen-type Schiff base ligand, (*E*)-2-{[(2-aminopyridin-3-yl)imino]methyl}-4,6-di-*tert*-butylphenol (HL), are reported. The characterization has been carried out using X-ray single crystallographic, thermogravimetric, and spectroscopic techniques. The complex has been combined with polyvinyl chloride (PVC) membrane of various compositions and tested as an electrochemical electrode towards recognition of several anions. The electrode exhibits exceptional electrochemical recognition for the nitrite (NO_2^-) anion in aqueous media. The electrode exhibited a linear response to NO_2^- with a detection limit of 5.76 μM and displayed a linear Nernstian slope over the nitrite concentration range of 1.0×10^{-5}–1.0×10^{-1} M in the pH range of 3–7 and a fast response time of less than 10 seconds. Theoretical calculations showed that the sensing could be via anion exchange in the Co(III) complex.

Keywords. Schiff base; nitrite; anion sensor; electrochemical recognition; salphen ligand.

1. Introduction

Designing anion selective receptors has drawn great scientific attention over the recent years.[1–4] The sensing is basically an observable response of the receptor upon interacting with an anion, which can be done by a variety of mechanisms including but not limited to chromatographic,[5–9] optical (spectroscopic),[10–15] and electrochemical methods.[16–20]

The nitrite ion (NO_2^-) plays a significant role in producing toxic, mutagenic and carcinogenic N-nitosamines; in producing NO, which is a diverse and potent biological messenger;[21–23] and as a food preservative.[24–26] Thus, determination of the nitrite anion at the trace levels is still a great deal of interest.[27]

Salphen and salen-type ligands and their corresponding metal complexes, apart from applications such as intercalation to the DNA base pairs,[28] have the potential use for potentiometric detections of biologically and environmentally common anions.[29] Malinowski and coworkers showed a highly fluoride (F^-) selective electrode by a Zr^{2+} complex of salphen type ligands.[30] There are several other potentiometric anion selective electrodes including the nitrite anion. The metal complexes of phthalocyanine, porphyrin and carbazole rings are a few examples of ionophores for the nitrite anion. These types of sensors suffer from either having narrow linear ranges, having higher detection limits or having interference from other anions.[31] Thus, there are still scientific efforts to develop potentiometric nitrite sensors with lower detection limits and more selective toward the nitrite ion. Recently, Ganjali *et al.,* reported for the first time that salphen-type ligands can also be used as nitrite sensors.[27]

Herein, we report experimental and computational studies of the Co(III) complex of the HL ligand, including synthesis and characterization to the potentiometric nitrite selective electrode application.

*For correspondence

Electronic supplementary material: The online version of this article (doi:10.1007/s12039-017-1363-6) contains supplementary material, which is available to authorized users.

2. Experimental and Computational Methods

2.1 *Reagents*

For the synthesis and characterization, all chemicals and solvents were purchased from commercial suppliers (Aldrich or Merck) and used with no more purification unless otherwise specified.

For the anion recognition application studies, the reagents used for the preparation of the electrode membrane, tetrahydrofuran (THF), graphite, high molecular weight poly(vinyl chloride) (PVC), dioctyl sebacate (DOS), sodium tetraphenylborate (NaTPB) and potassium tetrakis (p-chlorophenyl)borate (KTClPB) were obtained from Fluka (Bucks, Switzerland). Hardener (Desmodur RFE) and epoxy (Macroplast Su 2227) were obtained from Bayer AG (Darmstadt, Germany) and Henkel (Istanbul, Turkey). All aqueous solutions were prepared with salts of the highest purity available using freshly deionized water. For each anion, 10^{-1} mol L^{-1} stock solutions were prepared by using sodium salts. The dilute solutions (10^{-2}–10^{-7} mol L^{-1}) were prepared by dilution of the stock standard solutions.

2.2 *Apparatus*

The ^{1}H-NMR spectrum was recorded on a Bruker AVANCE III 400 MHz NMR spectrometer (Germany). The sample was dissolved in $CDCl_3$ using tetramethylsilane as an internal standard. The IR spectra were recorded on a Perkin Elmer Spectrum 100 spectrometer in the range 4000–600 cm^{-1}. The MALDI-TOF-MS spectra on a Microflex LT spectrometer were recorded in ethanol with no matrix. The elemental analysis measurements were performed on a LECO CHNS-932 elemental analyzer (USA). The thermal analysis of HL was recorded on a TGA/SDTA-851 instrument, within 25–700°C temperature range, in argon atmosphere at a heating rate of 10°C/min. The thermal analysis measurement of Co(III) complex was conducted with a Perkin Elmer Pyris 1 TGA thermal analyser (USA), within 50–700°C temperature range, in static air atmosphere at a heating rate of 20°C/min.

A computer-controlled, laboratory-built, high-input impedance eight-channel potentiometric system was used for the potentiometric measurements. The measurement system used a home-made software to observe the potentiometric response of the prepared electrodes. A saturated Ag-AgCl reference electrode (Gamry) was used as the reference electrode, throughout the potentiometric measurements. A glass pH electrode (Schott) with a Jenway 3040 model Ion Analyzer was used for the pH measurements. An Ultrasonic LC30 stirrer (Germany) was used for the homogenization of the prepared and diluted solutions. ElgaPureLab Option Q Water Purification System was used for the purification of the water.

2.3 *Synthesis*

The HL ligand was synthesized by the condensation of 2,3-diaminopyridine with 3,5-di-*tert*-butyl-2-hydroxybenzaldehyde. The procedure for the synthesis of HL was described elsewhere.[32–35] The Co(III) complex was synthesized using this ligand.

2.3a *Synthesis of HL*: A 30 mL ethanol-methanol (2:1, v/v) solution of 3,5-di-*tert*-butyl-2-hydroxybenzaldehyde (0.47 g, 2 mmol) was gradually added to a 30 mL ethanol-methanol (2:1, v/v) solution of 2,3-diaminopyridine (0.22 g, 2 mmol). The mixture was refluxed for 5 h and stirred for 16 h at room temperature. Then it was filtered and the precipitate formed after standing was washed with methanol, diethyl ether and dried in air. The yellow product was obtained. Yield: 60%. ^{1}H-NMR spectrum (400 MHz; $CDCl_3$), δ/ppm: 13.0 [s, OH]; 8.6 [s, CH_{imine}]; 8.0–6.7 [m, CH_{Ar}]; 4.8 [s, NH_2]; 1.5 [s, $C(CH_3)_3$]; 1.3 [s, $C(CH_3)_3$]. IR spectrum, ν, cm^{-1}:3469 ν(O-H); 3259-3134 $\nu(NH_2)$; 2959 ν(C-H); 1607 ν(C=N); 1588 ν(C=C). MALDI-TOF-MS spectrum m/z: 325. Found, %: C 73.98; N 11.51; H 8.46. Calculated ($C_{20}H_{27}N_3O$), %: C 73.81; N 12.91; H 8.36.

2.3b *Synthesis of Co(III) complex*: A 30 mL ethanol solution of $Co(NO_3)_2{\cdot}6H_2O$ (0.29 g, 1 mmol) was added dropwise to a 30 mL ethanol solution of HL (0.65 g, 2 mmol). The mixture was refluxed for 3 h and stirred for 8 h at room temperature. Then it was filtered and brown crystals suitable for X-ray diffraction were obtained by slow evaporation of the solvent. Yield: 50%. IR spect-rum, ν, cm^{-1}:3372 ν(O-H); 2957 ν(C-H); 1610 ν(C=N); 1578 ν(C=C). MALDI-TOF-MS spectrum m/z: 708 (complex ion, $[CoL_2]^+$). Found, %: C 59.20; N 12.07; H 6.60. Calculated for $[CoL_2]NO_3{\cdot}2H_2O$ ($C_{40}H_{56}CoN_7O_7$), %: C 59.62; N 12.17; H 7.00.

2.4 *X-ray data collection and structure refinement*

Data were obtained with a Bruker APEX II QUAZAR three-circle diffractometer. Indexing was performed using APEX2.[36] Data integration and reduction were carried out with SAINT.[37] Absorption correction was performed by multi-scan method implemented in SADABS.[38] The structure was solved and refined using Bruker SHELXTL software package.[39] The H atoms bound to the aromatic and aliphatic C atoms were positioned geometrically and refined using a riding mode. The H atoms bound to the N atoms were placed in calculated positions. For the cobalt(III) complex, the unit cell consists of badly disordered solvents which could not be modelled as discrete atomic sites. Herein, the contributions of the seriously disordered solvent molecules were eliminated from the structure using SQUEEZE in PLATON[40] program suite. Crystal structure validations and geometrical calculations were performed using PLATON.[40] MERCURY software[41] was used for visualization of the crystallographic information file (cif).

2.5 *Preparation of electrodes*

Nitrite-selective PVC-based membrane solid contact electrodes were prepared in the same manner as described in our previous work.[42] The electrodes were prepared in two steps. In the first step, a conductive solid contact was prepared by using an appropriate mass ratio of graphite, epoxy and hardener. A shielded copper wire, 0.5 mm in diameter and 15.0 cm in length was dipped into conductive mixture for a few times to obtain a solid contact with a coating thickness of about 0.2 mm and then dried at room temperature for 1 day to evaporate THF, leaving the solid contact layer coating the wire. In the second step, 250 mg membrane cocktail was prepared by dissolving polymeric membrane components, ionophore, PVC and DOS {bis(2-ethylhexyl) sebacate} at different ratios in 3.0 mL THF. The surface of the conductive solid contact was coated with the membrane cocktail by dipping the coated copper wire into the cocktail 4–5 times. Then, the membrane coated electrode surface was left to be dried in laboratory conditions overnight. The prepared electrodes were equilibrated in 0.1 M nitrite solution for 24 h and used further for potential measurement studies. The used electrodes were equilibrated before each measurement process for about half an hour to obtain stable emf readings.

2.6 *Electrochemical measurement protocol*

All electromotive forces (emf) were recorded at room temperature in stirred solutions with the following cell assembly: SC-ISE |test solution| Ag-AgCl, KCl (sat'd). The cell consists of SC-ISE (ion selective electrode) as the indicator electrode, a saturated Ag-AgCl reference electrode. The performance of the prepared electrodes was examined by measuring the emf's of sodium nitrite solutions prepared in the concentration range 10^{-1}–10^{-6} mol/L by serial dilutions. Prepared electrodes and reference electrode were washed with deionized water and dried with an adsorbent paper before changing the test solutions. Each measurement was performed simultaneously on three electrodes from the same mother membrane.

2.7 *Theoretical calculations*

All the calculations were carried out in the gas phase using Gaussian 09 program.[43] In the calculations, no restrictions have been applied. All the geometries for $[CoL_2]^+$, free X^- (NO_3^- and NO_2^-) ions and the $[CoL_2]X$ complexes were relaxed to their minimum energies without freezing any atom or applying any restriction. In addition, symmetry constraints were also removed from all the calculations. All optimizations were confirmed for their minima by frequency calculations.

The initial geometry of $[CoL_2]^+$ was retrieved by removing the counter ion atoms from the crystal structure of the cobalt(III) complex. The initial coordinates of the nitrate anion were generated from its position in the crystal structure of the cobalt(III) complex. We have generated several starting structures for $[CoL_2]NO_2$ by removing one of the oxygen atoms from the counter ion of $[CoL_2]NO_3$ each time and changing the distance of NO_2^- from the Co^{3+} cation. These possible structures of $[CoL_2]NO_2$ were separately calculated and the minimum energy structure was used in comparison to $[CoL_2]NO_3$.

In spite of the difficulty of the most DFT calculations for predicting long distance interactions, recent studies have been successfully performed to describe the covalency along with long range interactions including the π–π stacking interaction and hydrogen bonding.[44–49] In particular, M06-2X[45–49] is widely used for its capability of describing hydrogen bonding as well as π–π stacking interactions.[28]

Thus, we used M06-2X and B3LYP with Grimme's dispersion functions in the calculations. In order to ease the computational cost, we used the following generic basis set: 6-311++G(d,p) for Co^{3+}, 6-31+G(d) for the ligands coordinating to the Co^{3+} ion and 3-21G for the *tert*-butyl groups on the ligands.

3. Results and Discussion

3.1 *Characterization of synthesized compounds*

3.1a ^{1}*H-NMR spectroscopy*: In the spectrum of HL, the singlets observed at 13.0 ppm and 4.8 ppm are due to the chemical shifts of the -OH and -NH_2 protons, respectively. Other observed peaks in the spectrum belong to the CH protons including the azomethine proton (-CH=N-), the singlet at 8.6 ppm, and the *tert*-butyl groups, the multiplet at 1.5 and 1.3 ppm. The signals of the aromatic protons appeared at 8.0 - 6.7 ppm (Figure S1 in Supplementary Information).

3.1b *IR spectroscopy*: The IR spectrum of HL (Figure S2 in Supplementary Information) shows several bands in the region of 4000 and 1500 cm^{-1}. Among these, the band at 3469 cm^{-1}, the doublet at 3259–3134 cm^{-1} and the band at 2959 cm^{-1} were assigned as the stretch modes of the -OH, -NH_2 and -CH groups, respectively. The peaks at 1607 and 1588 cm^{-1} were assigned as C=N and C=C stretching frequencies, respectively.

Upon formation of the complex, a new broad band peaking at 3372 cm^{-1} and suppressing -NH_2 stretches was appeared, which is most likely due to the –OH stretches of the crystal water molecules (Figure S3 in Supplementary Information). The –C-H stretches were almost unaffected by the complexation. The C=N and C=C stretching vibrations were also observed at 1610 and 1578 cm^{-1}.

3.1c *Mass spectroscopy*: The MALDI-TOF-MS spectrum of HL shows the molecular ion peak at m/z: 325 (Figure S4 in SI). The characteristic molecular ion peak

of $[CoL_2]^+$ was observed at m/z: 708, confirming the formation of the $[CoL_2]^+$ complex ion (Figure S5 in SI).

3.1d *Thermogravimetric (TG) analysis*: Figure 1a shows the plot of the relative weight loss against increasing temperature for the HL ligand. The HL ligand is stable up to 96°C and the thermal decomposition of HL takes place in two main stages. The first decomposition occurs between the temperatures of 96°C and 163°C. This stage corresponds to the elimination of the pyridin-2-amine ($C_5H_6N_2$) residue from HL (calc. 28.9%; exp. 28.4%). The intermediate product remains stable from 163°C to 180°C. The second decomposition starts at 180°C and continues up to 345°C. This stage is related to the decomposition of the remaining organic residue. A little organic sediment remained at the end of the decomposition process since heating was carried out in argon atmosphere.

The TG plot of the Co(III) complex in Figure 1b, on the other hand, shows that the complex starts to decompose at ~70°C and this first decomposition continues up to ~150°C. At this stage, the crystal water molecules were removed from the complex (calc. 4.5%; exp. 4.1%). The remaining anhydrous complex has another weight loss in the range of ~230°C and ~420°C. However, a stable intermediate with a fixed weight plateau did not occur in this decomposition step just because

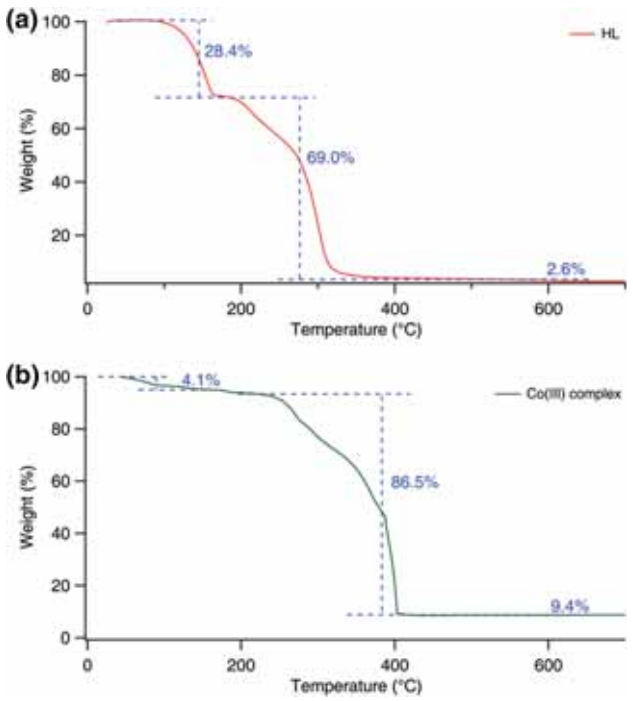

Figure 1. Thermogravimetric plot of (a) HL in argon atmosphere, and (b) Co(III) complex in air atmosphere. The dashed lines and labels represent the weight loss in each step.

further reactions for a complete decomposition were initiated. It is most likely that Co_2O_3 is the final remainder of the decomposition process in static air atmosphere (calc. 10.3%; exp. 9.4%).

3.2 *Crystallographic analysis*

Crystallographic data and refinement details of the Co(III) complex are given in Table 1. Single crystal X-ray diffraction analysis reveals that the complex crystallizes in the monoclinic space group, $P2_1/n$. The asymmetric unit comprises of nearly identical two independent $[CoL_2]^+$ and a nitrate counter ion. The Co^{3+} ion is coordinated to two O atoms of the phenolate groups, two N atoms of the free $-NH_2$ groups and two N atoms of the –CH=N– groups in the ligands in a distorted octahedral environment (Figure 2).

In the CoN_4O_2 coordination sphere, the Co-N bond lengths range from 1.889(4) Å for Co1-N4 to 1.975(5) Å for Co1-N3, and the Co-O bond lengths range from 1.865(4) Å for Co1-O2 to 1.877(3) Å for Co2-O7 (Table 2). These bond lengths are comparable to those reported for corresponding cobalt complexes with Schiff base ligands.[50–53] The N-Co-N, O-Co-O, and N-Co-O bond angles are within the range of 84.0(2)° and 179.11(19)°.

3.3 *Application of the Co(III)-salphen complex as an ionophore*

The Co(III)-salphen complexes have the potential application as ionophores for nitrite ion-selective electrodes by inducing the non-Hofmeister selectivity pattern. Thus, we examined the complex by preparing a nitrite selective membrane electrode. The critical response characteristics of the solid contact nitrite-selective electrode were systematically assessed according to the International Union of Pure and Applied Chemistry, IUPAC, recommendations.[54,55]

The preparation of the solid contact electrodes is discussed in section 2.5. We performed potentiometric measurements to assess the potentiometric response of the prepared electrodes toward some common anions in the activity (α) range of 1.0×10^{-1}–1.0×10^{-6} M by serial dilution. The electrodes with Co(III) complex as ionophore showed anionic potentiometric responses. Figure 3 shows the Nernstian plots of the potentiometric responses obtained for different anions. The best analytical potentiometric responses in terms of detection limits and the linearity of the slopes were obtained for nitrite anion.

The selectivity and sensitivity of the membrane electrode are significantly related with the ionophore

Table 1. X-ray crystallographic data and refinement parameters for the Co(III) complex.

Formula of refinement model	$C_{80}H_{104}Co_2N_{13}O_7$
Formula weight ($g \cdot mol^{-1}$)	1477.62
Temperature (K)	100(2)
Wavelength (Å)	0.71073
Crystal system	Monoclinic
Space group	$P2_1/n$
a(Å)	18.1040(9)
b(Å)	16.9425(9)
c(Å)	30.9367(15)
α(°)	90
β(°)	102.110(3)
γ(°)	90
Crystal size (mm)	0.31 × 0.35 × 0.40
V ($Å^3$)	9278.0(8)
Z	4
ρ_{calc} ($g \cdot cm^{-3}$)	1.058
μ (mm^{-1})	0.409
F(000)	3140
θ range for data collection (°)	2.95 - 25.00
h/k/l	−14 <= h <= 21, −20 <= k <= 16, −35 <= l <= 36
Reflections collected	66194
Independent reflections	15402 [R(int) = 0.0662]
Data/restraints/parameters	15402 / 60 / 943
Goodness-of-fit on F^2	1.089
Final R indices [I > 2σ(I)]	$R_1 = 0.0980$, $wR_2 = 0.2732$
R indices (all data)	$R_1 = 0.1599$, $wR_2 = 0.2961$
Largest diff. peak and hole ($e \cdot Å^{-3}$)	1.147 and -0.724

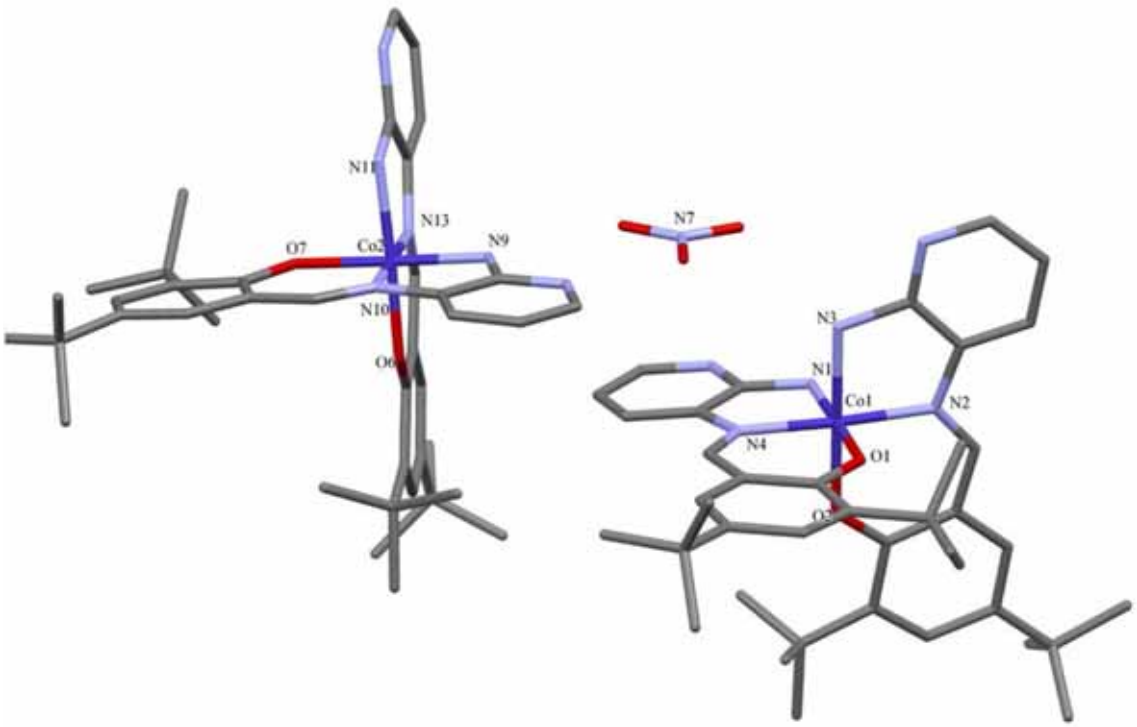

Figure 2. The asymmetric unit of the Co(III) complex. The H atoms were omitted for clarity.

Table 2. Selected bond lengths (Å) and bond angles (°) for the Co(III) complex.

Bond lengths (Å)					
Co1-N1	1.902(5)	Co1-O1	1.869(4)	Co2-N11	1.965(5)
Co1-N2	1.898(5)	Co1-O2	1.865(4)	Co2-N13	1.891(5)
Co1-N3	1.975(5)	Co2-N9	1.905(5)	Co2-O7	1.877(3)
Co1-N4	1.889(4)	Co2-N10	1.906(5)	Co2-O6	1.873(4)
Co1-N7	4.555(6)	Co2-N7	5.539(2)	Co2-Co1	8.962(4)
Bond angles (°)					
O2-Co1-O1	90.27(17)	O2-Co1-N4	87.82(18)	O1-Co1-N4	95.13(18)
O2-Co1-N2	94.3(2)	O1-Co1-N2	87.4(2)	N4-Co1-N2	176.7(2)
O2-Co1-N1	89.6(2)	O1-Co1-N1	179.11(19)	N4-Co1-N1	84.0(2)
N2-Co1-N1	93.5(2)	O2-Co1-N3	178.3(2)	O1-Co1-N3	88.10(19)
N4-Co1-N3	92.10(18)	N2-Co1-N3	85.9(2)	N1-Co1-N3	92.0(2)
O6-Co2-O7	90.21(17)	O6-Co2-N13	94.6(2)	O7-Co2-N13	86.87(17)
O6-Co2-N9	90.7(2)	O7-Co2-N9	179.1(2)	N13-Co2-N9	93.0(2)
O6-Co2-N10	87.4(2)	O7-Co2-N10	94.5(2)	N13-Co2-N10	177.6(2)
N9-Co2-N10	85.6(2)	O6-Co2-N11	177.67(19)	O7-Co2-N11	87.83(17)
N13-Co2-N11	86.6(2)	N9-Co2-N11	91.3(2)	N10-Co2-N11	91.5(2)

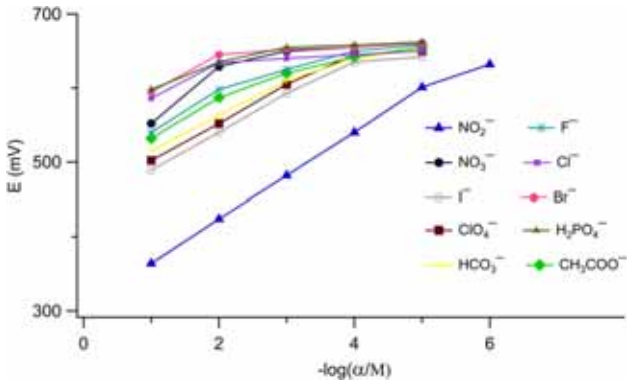

Figure 3. Potentiometric responses for different anions. The interfering SCN^- anion is omitted from the graph for better appearance purposes.

concentration, the nature of the solvent mediator, the plasticizer/PVC ratio, and the nature of additives. We have tried several different membrane compositions in order to optimize the electrode (Table 3). Since earlier studies showed that the nitrite selective membranes were prepared with DOS {bis(2-ethylhexyl) sebacate} to exhibit the lowest limit of detection, we only tested the DOS as the plasticizer.[27,56] The sensitivity of the electrode increases with increasing ionophore concentration up to 2%. Further addition of ionophore resulted in performance loss of the electrode. Table 3 also shows the effect of ionic additives of NaTPB and KTClPB on the potential responses of the electrodes. The presence of an additive generally improves the performance characteristics of the membrane electrode. However, the comparison of the two additives shows that NaTPB is more effective than KTClPB. By the addition of 0.5% NaTPB, the slope of the potential sensor response increases from a sub-Nernstian value of 52 mV/decade (run 3) to a Nernstian value of 59.1 mV/decade (run 6). The best analytical potentiometric responses of the nitrite anion were obtained in the composition of 2% (w/w) ionophore, 32% (w/w) PVC, 65.5% (w/w) DOS and 0.5% (w/w) NaTPB (the run number 6 in Table 3). Therefore, we carried out further studies with this optimum electrode composition.

Table 3. Membrane compositions and the corresponding responses in ligand-based nitrite-selective electrodes.

Run	Composition, % (mass, w/w)					Detection limit (M)	Linear range (M)	Slope (mV/decade)
	Ligand	PVC	DOS	NaTPB	KTClPB			
1	1	32	67			9.94×10^{-5}	1×10^{-1}–1×10^{-5}	47.97
2	1.5	32	66.5			8.85×10^{-6}	1×10^{-1}–1×10^{-5}	50.62
3	2	32	66			7.22×10^{-6}	1×10^{-1}–1×10^{-5}	52.45
4	2.5	32	65.5			9.85×10^{-6}	1×10^{-1}–1×10^{-5}	49.35
5	2	32	65.5		0.5	9.12×10^{-6}	1×10^{-1}–1×10^{-5}	54.42
6	2	32	65.5	0.5		5.76×10^{-6}	1×10^{-1}–1×10^{-5}	59.20
7	2	32	65	1.0		6.14×10^{-6}	1×10^{-1}–1×10^{-5}	52.20

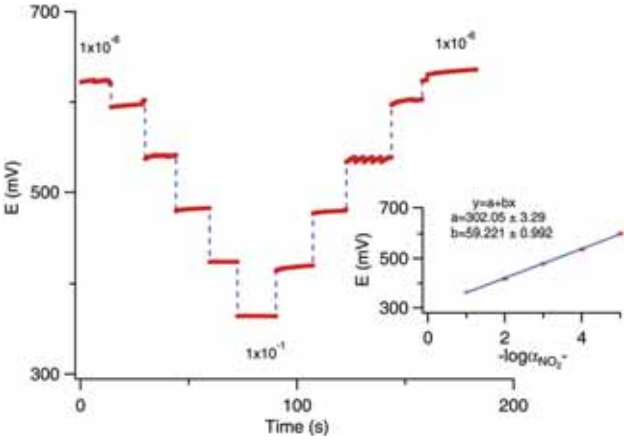

Figure 4. Potentiometric responses and calibration plot of the prepared electrode for the NO_2^- ions at different concentrations.

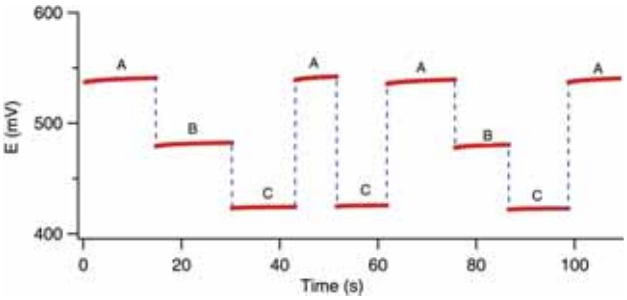

Figure 5. Reproducibility of the electrode at three NO_2^- concentrations, A: 1.0×10^{-4} M, B: 1.0×10^{-3} M, C: 1.0×10^{-2} M.

The potentiometric response of the electrode toward NO_2^- was recorded in aqueous solutions of NO_2^- in the concentration range of 1.0×10^{-6}–1.0×10^{-1} M. The calibration curve for related potentiometric signals was plotted and shown in Figure 4. The electrode shows a linear response in the concentration range of 1.0×10^{-5}–1.0×10^{-1} M ($R^2 = 0.9996$) with a slope of −59.20 mV/decade. The detection limit of the electrode was calculated by using the intersections of the two extrapolated segments of the calibration plot as 5.76×10^{-6} M. The response time of the electrode was determined as 10 seconds.

The reproducibility of the electrode potential measurements was also investigated by changing nitrite concentration back and forth among 1×10^{-4} M, 1×10^{-3} M and 1×10^{-2} M (Figure 5). The average potential values and their standard deviations for these three concentrations were calculated as 540.2 ± 0.8, 482.4 ± 0.9 and 424.1 ± 0.6, respectively. The results indicate that the prepared electrode has a good reproducibility for the analytical measurement purposes.

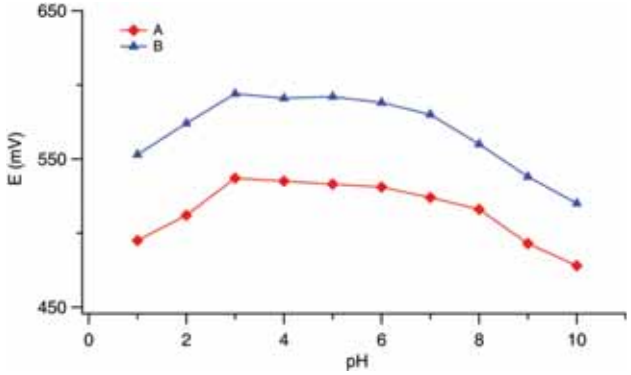

Figure 6. pH dependence of the potentiometric response of the NO_2^- selective electrode, A: 1.0×10^{-4} M, B: 1.0×10^{-5} M.

We also investigated the effect of pH on the sensing capability of the electrode. To achieve this, we prepared two test solutions of NO_2^- with concentrations of 1×10^{-4} and 1×10^{-5} M in the phosphate buffers with pH values ranging between 1 and 10. The response of the prepared electrode persisted constant and robust in the pH range of 3.0–7.0 in both test solutions (Figure 6). The notable decrease in pH below 3.0 might be due to the responsive behavior of the electrode toward oppositely charged H_3O^+ ion. The sharp decrease in electrode potential above pH 7.0 may be ascribed to the potentiometric response of the electrode to OH^- ion.

The potentiometric selectivity is one of the most demanded features for an ideal electrode. Here, we used the separate solution method (SSM) for the calculation of the selectivity coefficients.[57] In this method, logα vs. E relations of an ISE for the primary and interfering ions are obtained independently. Then, the activities that correspond to the same electrode potential value are used to determine the $K_{A,B}^{pot}$ value by using the following equation:

$$K_{A,B}^{pot} = \frac{a_A}{(a_B)^{z_A/z_B}} \quad (1)$$

where, α_A and α_B are the activities (mol/L); z_A and z_B are the charge states of primary (NO_2^- in our case) and interfering ions, respectively.

The Nikolsky coefficient is determined using SSM by comparing two solutions, each containing a salt of the primary and interfering ion only.[57] The resulting values of the selectivity coefficients are given in Table 4. According to the table, the ranking among the anions is different from the Hofmeister series and most of the anions would not affect the selectivity of the prepared sensor. The prepared solid contact sensor can act as selective toward NO_2^- ions, however, very lipophilic ions such as SCN^- still exhibit major interference.

Table 4. Potentiometric selectivity coefficients calculated according to SSM for NO_2^- selective electrode.

Interference	$\log\left(K^{pot}_{NO_2^-,X}\right)$
SCN^-	0.18
I^-	−2.12
ClO_4^-	−2.34
HCO_3^-	−2.56
CH_3COO^-	−2.85
F^-	−2.98
NO_3^-	−3.19
Cl^-	−3.76
Br^-	−3.91
$H_2PO_4^-$	−3.97

3.4 *DFT calculations*

Since the first coordination shell of the Co^{3+} ion is fully completed by the strong chelating ligands in an octahedral geometry, we theoretically explored the plausibility of sensing mechanism to be based on a reversible exchange of the NO_3^- with NO_2^- anion. In order to accomplish this, we carried out several DFT optimization calculations on both $[CoL_2]NO_3$ and $[CoL_2]NO_2$ in which the anions are replaced in the outer sphere of the Co^{3+} ion (Figure 7). The results are qualitatively consistent with experimental data. Table 5 shows the predicted binding energies along with the basis set superposition (BSSE) and zero point vibrational energy corrections (ZPVE). The binding energies, ΔE_{bind} were calculated based on the following equation:

$$\Delta E_{bind} = E_C - (E_{rec} + E_{anion}) \quad (2)$$

where E_C, E_{rec}, and E_{anion} are the energy terms of the optimized structures for the receptor-anion complex, receptor and isolated anion in the gas phase, respectively. The smaller sized NO_2^- has a greater affinity to $[CoL_2]^+$ by ∼8 kcal/mol.

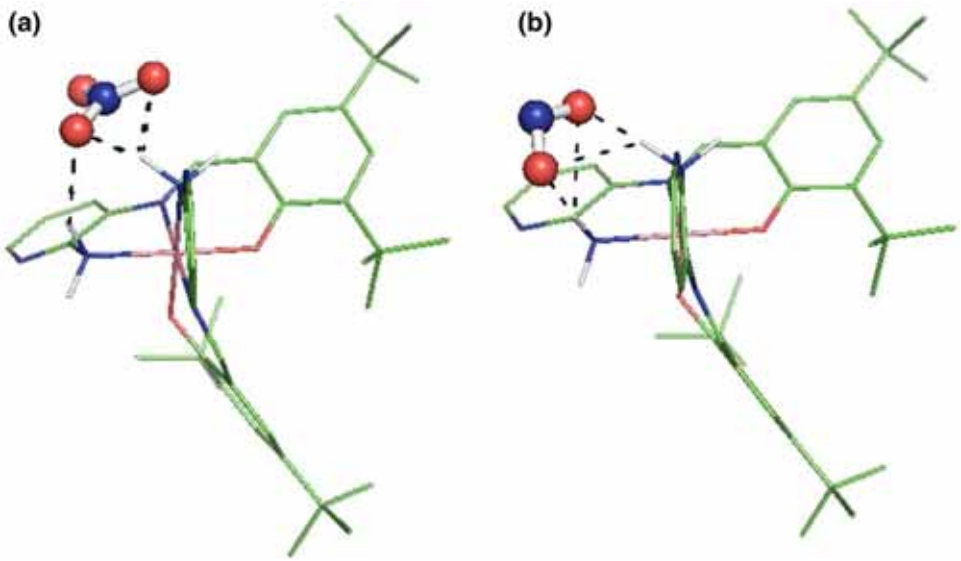

Figure 7. Optimized structures using M06-2X and the generic basis set described in Section 2.7 for a) $[CoL_2]NO_3$ and b) $[CoL_2]NO_2$. Nonpolar H atoms are not shown for clarity.

Table 5. The calculated binding energies (kcal/mol) of both NO_3^- and NO_2^- anions to $[CoL_2]^+$ receptor in gas phase along with ZPVE and BSSE corrections using M06-2X and B3LYP-D3 with the generic basis set described in section 2.7. $\Delta\Delta E = \Delta E_{NO2-} - \Delta E_{NO3-}$.

	M06-2X			B3LYP-D3		
	SCF	SCF (+BSSE)	SCF (+BSSE +ZPVE)	SCF	SCF (+BSSE)	SCF (+BSSE +ZPVE)
ΔE_{NO3-}	−93.98	−91.74	−90.80	−84.63	−82.57	−81.72
ΔE_{NO2-}	−101.51	−99.39	−98.90	−91.88	−89.74	−89.05
$\Delta\Delta E$	−7.53	−7.65	−8.10	−7.25	−7.17	−7.34

It should be noted that these binding energies belong to the minimum energy structures. We have found several other local minima for the proposed nitrite containing complex and one more local minimum for the nitrate containing complex (Figures S6-S8 in Supplementary Information). However, the binding affinities of the nitrite anion to the $[CoL_2]^+$ receptor in all the calculations were still greater than those of the nitrate anion.

4. Conclusions

In this study, we synthesized and characterized a new Co(III) complex of a salphen derivative Schiff base ligand. We used this complex as an ionophore for the application of electrochemical sensors. For that, we designed PVC-based membrane solid contact electrodes with this ionophore and tested their usage as an electrode for several anions. Among the anions, nitrite (NO_2^-) showed a linear Nernstian slope over the studied concentration range. The detection limit of the prepared electrode was calculated as 5.76 μM for NO_2^-. In agreement with the experiments, the DFT calculations on the binding mode showed that a exchange of anions is plausible.

Supplementary Information (SI)

Crystallographic data for the structural analysis of Co(III) complex has been deposited with the Cambridge Crystallographic Data Centre bearing the CCDC number 1517539. Copy of this information is available on request at free of charge from CCDC, Union Road, Cambridge, CB21EZ, UK (fax: +44-1223-336-033; e-mail: deposit@ccdc.ac.uk or http://www.ccdc.cam.ac.uk). The ^{1}H-NMR spectrum of the HL ligand, the FT-IR spectra of the HL ligand and Co(III) complex, the mass spectra of the HL ligand and Co(III) complex, two optimized structures of $[CoL_2]NO_3$ overlapped, the optimized structures of $[CoL_2]NO_2$ overlapped, and the minimum energy structures of $[CoL_2]NO_3$ and $[CoL_2]NO_2$ along with the crystal structure of $[CoL_2]NO_3$ overlapped (Figures S1–S8) are available at www.ias.ac.in/chemsci.

Acknowledgements

We gratefully acknowledge Ricardo B. Metz from the University of Massachusetts for allowing to use computer clusters and software packages in the calculations; Serkan Demir and Omer Andac from Ondokuz Mayis University for their valuable advice. The numerical calculations reported in this paper were partially performed at TUBITAK ULAKBIM, High Performance and Grid Computing Center (TRUBA resources).

References

1. Busschaert N, Caltagirone C, Van Rossom W and Gale P A 2015 Applications of Supramolecular Anion Recognition *Chem. Rev.* **115** 8038
2. Gale P A and Caltagirone C 2015 Anion sensing by small molecules and molecular ensembles *Chem. Soc. Rev.* **44** 4212
3. Kim D S and Sessler J L 2015 Calix[4]pyrroles: versatile molecular containers with ion transport, recognition, and molecular switching functions *Chem. Soc. Rev.* **44** 532
4. Vargas Jentzsch A 2015 Applications of halogen bonding in solution *Pure Appl. Chem.* **87** 15
5. Kodamatani H, Yamazaki S, Saito K, Tomiyasu T and Komatsu Y 2009 Selective determination method for measurement of nitrite and nitrate in water samples using high-performance liquid chromatography with post-column photochemical reaction and chemiluminescence detection *J. Chromatogr. A* **1216** 3163
6. Kumar Malik A and Faubel W 2000 Capillary electrophoretic determination of zinc dimethyldithiocarbamate (Ziram) and zinc ethylenebisdithiocarbamate (Zineb) *Talanta* **52** 341
7. Royall P G, Craig D Q, Price D M, Reading M and Lever T J 1999 An investigation into the use of micro-thermal analysis for the solid state characterisation of an HPMC tablet formulation *Int. J. Pharm.* **192** 97
8. Helaleh M I H and Korenaga T 2000 Ion chromatographic method for simultaneous determination of nitrate and nitrite in human saliva *J. Chromatogr. B* **744** 433
9. Croitoru M D 2012 Nitrite and nitrate can be accurately measured in samples of vegetal and animal origin using an HPLC-UV/VIS technique *J. Chromatogr. B* **911** 154
10. Afkhami A, Bahram M, Gholami S and Zand Z 2005 Micell-mediated extraction for the spectrophotometric determination of nitrite in water and biological samples based on its reaction with p-nitroaniline in the presence of diphenylamine *Anal. Biochem.* **336** 295
11. Aydın A, Ercan Ö and Taşcıoğlu S 2005 A novel method for the spectrophotometric determination of nitrite in water *Talanta* **66** 1181
12. Senra-Ferreiro S, Pena-Pereira F, Lavilla I and Bendicho C 2010 Griess micro-assay for the determination of nitrite by combining fibre optics-based cuvetteless UV-vis micro-spectrophotometry with liquid-phase microextraction *Anal. Chim. Acta* **668** 195
13. Martinez-Tome M J, Esquembre R, Mallavia R and Mateo C R 2010 Development of a dual-analyte fluorescent sensor for the determination of bioactive nitrite and selenite in water samples *J. Pharm. Biomed. Anal.* **51** 484
14. Fang Y I, Ohata H and Honda K 2009 Fluorometric determination of nitrite with 2,3-diaminonaphthalene by reverse phase HPLC under alkaline conditions *J. Pharmacol. Toxicol. Methods* **59** 153
15. Fujii S, Tokuyama T, Abo M and Okubo A 2004 Fluorometric determination of sulfite and nitrite in aqueous samples using a novel detection unit of a microfluidic device *Anal. Sci.* **20** 209
16. Evans N H and Beer P D 2014 Advances in anion supramolecular chemistry: from recognition to chemical applications *Angew. Chem. Int. Ed. Engl.* **53** 11716

17. Shariar S M and Hinoue T 2010 Simultaneous voltammetric determination of nitrate and nitrite ions using a copper electrode pretreated by dissolution/redeposition *Anal. Sci.* **26** 1173
18. Gao Z, Wang G and Zhao Z 1990 Determination of trace amounts of nitrite by single-sweep polarography *Anal. Chim. Acta* **230** 105
19. Badea M, Amine A, Palleschi G, Moscone D, Volpe G and Curulli A 2001 New electrochemical sensors for detection of nitrites and nitrates *J. Electroanal. Chem.* **509** 66
20. Sharma B K, Shaikh A M, Chacko S and Kamble R M 2017 Synthesis, Spectral, Electrochemical and Theoretical Investigation of indolo[2,3-b]quinoxaline dyes derived from Anthraquinone for n–type materials *J. Chem. Sci.* **129** 483
21. Benjamin N, O'Driscoll F, Dougall H, Duncan C, Smith L, Golden M and McKenzie H 1994 Stomach NO synthesis *Nature* **368** 502
22. Lundberg J O, Weitzberg E, Lundberg J M and Alving K 1994 Intragastric nitric oxide production in humans: measurements in expelled air *Gut*. **35** 1543
23. Zweier J L, Wang P, Samouilov A and Kuppusamy P 1995 Enzyme-independent formation of nitric oxide in biological tissues *Nat. Med.* **1** 804
24. Lijinsky W and Epstein S S 1970 Nitrosamines as environmental carcinogens *Nature* **225** 21
25. Swann P F 1977 Carcinogenic risk from nitrite, nitrate and N-nitrosamines in food *Proc. R. Soc. Med.* **70** 113
26. Reddy D, Lancaster J R Jr. and Cornforth D P 1983 Nitrite inhibition of Clostridium botulinum: electron spin resonance detection of iron-nitric oxide complexes *Science* **221** 769
27. Ganjali M R, Shirvani-Arani S, Norouzi P, Rezapour M and Salavati-Niasari M 2004 Novel Nitrite Membrane Sensor Based on Cobalt(II) Salophen for Selective Monitoring of Nitrite Ions in Biological Samples *Microchim. Acta* **146** 35
28. Kocak A, Yilmaz H, Faiz O and Andac O 2016 Experimental and theoretical studies on Cu(II) complex of N,N'-disalicylidene-2,3-diaminopyridine ligand reveal indirect evidence for DNA intercalation *Polyhedron* **104** 106
29. Kleij A W, Kuil M, Lutz M, Tooke D M, Spek A L, Kamer P C J, van Leeuwen P W N M and Reek J N H 2006 Supramolecular zinc(II)-salphen motifs: Reversible dimerization and templated dimeric structures *Inorg. Chim. Acta* **359** 1807
30. Górski Ł, Saniewska A, Parzuchowski P, Meyerhoff M E and Malinowska E 2005 Zirconium(IV)-salophens as fluoride-selective ionophores in polymeric membrane electrodes *Anal. Chim. Acta* **551** 37
31. Parsaei M, Asadi Z and Khodadoust S 2015 A sensitive electrochemical sensor for rapid and selective determination of nitrite ion in water samples using modified carbon paste electrode with a newly synthesized cobalt(II)-Schiff base complex and magnetite nanospheres *Sens. Actuators, B* **220** 1131
32. Carreno A, Ladeira S, Castel A, Vega A and Chavez I 2012 (E)-2-[(2-Aminopyridin-3-yl)imino]methyl-4,6-di-tert-butylphenol *Acta Crystallogr. Sect. E* **68** o2507
33. Carreñoa A, Vegaa A, Zarateb X, Schottb E, Gacitúac M, Valenzuelac N, Preited M, Manríquezc J M and Chávezc I 2014 Synthesis, characterization and computational studies of (E)-2-[(2-aminopyridin-3-yl)imino]-methyl-4,6-di-tert-butylphenol *Quim. Nova* **37** 584
34. Carreno A, Gacitua M, Paez-Hernandez D, Polanco R, Preite M, Fuentes J A, Mora G C, Chavez I and Arratia-Perez R 2015 Spectral, theoretical characterization and antifungal properties of two phenol derivative Schiff bases with an intramolecular hydrogen bond *New J. Chem.* **39** 7822
35. Giannicchi I, Portalone G and Dalla Cort A 2013 Molecular aggregation of novel Zn(II)-salophenpyridyl derivatives *Supramol. Chem.* **25** 709
36. Bruker 2014 *APEX2* (Bruker AXS Inc.: Madison, WI, USA)
37. Bruker 2013 *SAINT* (Bruker AXS Inc.: Madison, WI, USA)
38. Bruker 2014 *SADABS* (Bruker AXS Inc.: Madison, WI, USA)
39. Bruker 2013 *SHELXTL* (Bruker AXS Inc.: Madison, WI, USA)
40. Spek A 2009 Structure validation in chemical crystallography *Acta Crystallogr. Sect. D* **65** 148
41. Macrae C F, Edgington P R, McCabe P, Pidcock E, Shields G P, Taylor R, Towler M and van de Streek J 2006 Mercury: visualization and analysis of crystal structures *J. Appl. Crystallogr.* **39** 453
42. Demir S, Yılmaz H, Dilimulati M and Andac M 2015 Spectral and thermal characterization of salophen type Schiff base and its implementation as solid contact electrode for quantitative monitoring of copper(II) ion *Spectrochim. Acta A* **150** 523
43. 58. Frisch M J, Trucks G W, Schlegel H B, Scuseria G E, Robb M A, Cheeseman J R, Scalmani G, Barone V, Mennucci B, Petersson G A, Nakatsuji H, Caricato M, Li X, Hratchian H P, Izmaylov A F, Bloino J, Zheng G, Sonnenberg J L, Hada M, Ehara M, Toyota K, Fukuda R, Hasegawa J, Ishida M, Nakajima T, Honda Y, Kitao O, Nakai H, Vreven T, Montgomery Jr. J A, Peralta J E, Ogliaro F, Bearpark M, Heyd J J, Brothers E, Kudin K N, Staroverov V N, Kobayashi R, Normand J, Raghavachari K, Rendell A, Burant J C, Iyengar S S, Tomasi J, Cossi M, Rega N, Millam J M, Klene M, Knox J E, Cross J B, Bakken V, Adamo C, Jaramillo J, Gomperts R, Stratmann R E, Yazyev O, Austin A J, Cammi R, Pomelli C, Ochterski J W, Martin R L, Morokuma K, Zakrzewski V G, Voth G A, Salvador P, Dannenberg J J, Dapprich S, Daniels A D, Farkas Ö, Foresman J B, Ortiz J V, Cioslowski J and Fox D J 2009 *Gaussian 09* (Wallingford CT: Gaussian, Inc.)
44. Swart M, van der Wijst T, Fonseca Guerra C and Bickelhaupt F M 2007 $\pi - \pi$ stacking tackled with density functional theory *J. Mol. Model.* **13** 1245
45. Biancardi A, Burgalassi A, Terenzi A, Spinello A, Barone G, Biver T and Mennucci B 2014 A Theoretical and Experimental Investigation of the Spectroscopic Properties of a DNA-Intercalator Salphen-Type ZnII Complex *Chem. Eur. J.* **20** 7439
46. Biancardi A, Biver T, Secco F and Mennucci B 2013 An investigation of the photophysical properties of minor

groove bound and intercalated DAPI through quantum-mechanical and spectroscopic tools *Phys. Chem. Chem. Phys.* **15** 4596
47. Robertazzi A, Magistrato A, de Hoog P, Carloni P and Reedijk J 2007 Density Functional Theory Studies on Copper Phenanthroline Complexes *Inorg. Chem.* **46** 5873
48. Spinello A, Terenzi A and Barone G 2013 Metal complex–DNA binding: Insights from molecular dynamics and DFT/MM calculations *J. Inorg. Biochem.* **124** 63
49. Lauria A, Bonsignore R, Terenzi A, Spinello A, Giannici F, Longo A, Almerico A M and Barone G 2014 Nickel(II), copper(II) and zinc(II) metallo-intercalators: structural details of the DNA-binding by a combined experimental and computational investigation *Dalton Trans.* **43** 6108
50. Lv S, Jie S and Li B-G 2015 Highly active and stereospecific polymerization of 1,3-butadiene catal yzed by bis[2-(4,5-diphenylimidazolyl)phenylimino]phe nolatecobalt(II) complexes *J. Organomet. Chem.* **799–800** 108
51. Alexopoulou K I, Zagoraiou E, Zafiropoulos T F, Raptopoulou C P, Psycharis V, Terzis A and Perlepes S P 2015 Mononuclear anionic octahedral cobalt(III) complexes based on *N*-salicylidene-o-aminophenol and its derivatives: Synthetic, structural and spectroscopic studies *Spectrochim. Acta A* **136** 122
52. Ghosh P, Chowdhury A R, Saha S K, Ghosh M, Pal M, Murmu N C and Banerjee P 2015 Synthesis and characterization of redox non-innocent cobalt(III) complexes of a O,N,O donor ligand: Radical generation, semi-conductivity, antibacterial and anticancer activities *Inorg. Chim. Acta* **429** 99
53. Gong D, Wang B, Jia X and Zhang X 2014 The enhanced catalytic performance of cobalt catalysts towards butadiene polymerization by introducing a labile donor in a salen ligand *Dalton Trans.* **43** 4169
54. Buck R P and Lindner E 1994 Recommendations for nomenclature of ionselective electrodes (IUPAC Recommendations 1994) *Pure Appl. Chem.* **66** 2527
55. Lindner E and Umezawa Y 2008 Performance evaluation criteria for preparation and measurement of macro-and microfabricated ion-selective electrodes (IUPAC Technical Report) *Pure Appl. Chem.* **80** 85
56. Crespo G A, Ghahraman Afshar M, Barrabés N, Pawlak M and Bakker E 2015 Characterization of Salophen Co(III) Acetate Ionophore for Nitrite Recognition *Electrochim. Acta* **179** 16
57. Umezawa Y, Bühlmann P, Umezawa K, Tohda K and Amemiya S 2000 Potentiometric selectivity coefficients of ion-selective electrodes. Part I. Inorganic cations (technical report) *Pure Appl. Chem.* **72** 1851